

A CRISPR/Cas9 screen identifies the histone demethylase MINA53 as a novel HIV-1 latency-promoting gene (LPG)

Huachao Huang^{1,†}, Weili Kong^{2,†}, Maxime Jean³, Guillaume Fiches², Dawei Zhou², Tsuyoshi Hayashi⁴, Jianwen Que¹, Netty Santoso^{2,*} and Jian Zhu^{2,*}

¹Department of Medicine, Columbia University Medical Center, New York, NY 10032, USA, ²Department of Pathology, The Ohio State University Wexner Medical Center, Columbus, OH 43210, USA, ³Department of Microbiology and Immunology, University of Rochester Medical Center, Rochester, NY 14642, USA and ⁴National Institute of Infectious Diseases, Tokyo 162-8640, Japan

Received January 10, 2019; Revised May 17, 2019; Editorial Decision May 23, 2019; Accepted May 24, 2019

ABSTRACT

Although combination antiretroviral therapy is potent to block active replication of HIV-1 in AIDS patients, HIV-1 persists as transcriptionally inactive proviruses in infected cells. These HIV-1 latent reservoirs remain a major obstacle for clearance of HIV-1. Investigation of host factors regulating HIV-1 latency is critical for developing novel antiretroviral reagents to eliminate HIV-1 latent reservoirs. From our recently accomplished CRISPR/Cas9 sgRNA screens, we identified that the histone demethylase, MINA53, is potentially a novel HIV-1 latency-promoting gene (LPG). We next validated MINA53's function in maintenance of HIV-1 latency by depleting MINA53 using the alternative RNAi approach. We further identified that *in vitro* MINA53 preferentially demethylates the histone substrate, H3K36me3 and that in cells MINA53 depletion by RNAi also increases the local level of H3K36me3 at LTR. The effort to map the downstream effectors unraveled that H3K36me3 has the cross-talk with another epigenetic mark H4K16ac, mediated by KAT8 that recognizes the methylated H3K36 and acetylated H4K16. Removing the MINA53-mediated latency mechanisms could benefit the reversal of post-integrated latent HIV-1 proviruses for purging of reservoir cells. We further demonstrated that a pan jumonji histone demethylase inhibitor, JIB-04, inhibits MINA53-mediated demethylation of H3K36me3, and JIB-04 synergizes with other latency-reversing agents (LRAs) to reactivate latent HIV-1.

INTRODUCTION

Combination antiretroviral therapy (cART) has significantly reduced HIV-1 associated morbidity and mortality (1,2). Nevertheless, cART is unable to completely eliminate HIV-1, and a subset of host cells is still latently infected with HIV-1 proviruses despite of treatment, mainly in resting CD4 T cells. These viral reservoirs are long-lived, self-replenishing and refractory to cART, although viral load in plasma level is under detectable level (3,4). Additionally, they contribute to residual viremia and viral rebound (5). They are characterized as having transcriptionally silent but inducible replication-competent proviruses that can lead to the production of infectious viruses when stimulated (6–8). Multiple host mechanisms have been proposed for establishment and maintenance of HIV-1 latency, well summarized elsewhere (9). Epigenetic silencing is definitely one critical step.

The 5' LTR of integrated HIV-1 proviruses contains the promoter/enhancer elements and is the center for epigenetic regulation of HIV-1 latency. There are two precisely positioned nucleosomes (nuc-0, nuc-1) in their basal repressed transcriptional state, which is separated by the nucleosome-free regulatory region including multiple transcription factor binding sites at 5' LTR (10). In particular, nuc-1 is located immediately downstream of the transcription start site, and it is highly suppressive to transcription and substantially remodeled once the latent HIV-1 proviruses is reactivated by external stimuli (11). For the integrated HIV-1 proviruses, their expression is subjected to the epigenetic regulation as other cellular genes, and influenced by the status of chromatin (euchromatin versus heterochromatin). The post-translational modification of the core histone proteins (H2A, H2B, H3, H4) forming the nucleosome is one of the key mechanisms that regulate the chromatin conden-

*To whom correspondence should be addressed. Tel: +1 614 293 4543; Fax: +1 614 292 7072; Email: Jian.Zhu@osumc.edu
Correspondence may also be addressed to Netty Santoso. Email: Netty.Santoso@osumc.edu

†The authors wish it to be known that, in their opinion, the first two authors should be regarded as Joint First Authors.

sation and determine the latent state of HIV-1 proviruses, mainly including histone methylation and acetylation (12). These histone modifications are critical for the accessibility of nuc-1, which can be pharmacologically targeted to reverse HIV-1 latency (13,14).

Histone acetylation is reversibly modified by the histone acetyltransferases (HATs) and histone deacetylases (HDACs). In general, HATs transfer the acetyl group to the lysine residues of histone proteins and promotes chromatin opening while HDACs remove the acetyl group and result in the repressive chromatin. Similarly, histone methyltransferases (HMTs) and histone demethylases (HDMs) oppositely and reversibly process histone methylation: HMTs are able to transfer 1–3 methyl groups to both lysine and arginine residues of histone proteins while HDMs remove these methyl groups. However, genetic consequence of histone methylation is more diverse than histone acetylation: methylated histones either repress or activate transcription, which really depends on which residue(s) of histones are methylated as well as what kind of methylation is on the residue(s). The relative activities of these epigenetic writers/erasers determine the ultimate level of histone markers, which can be recognized by readers, including chromatin remodelers and transcription factors, to execute their regulatory functions.

Therefore, multi-layered and comprehensive epigenetic regulations involving the multiple host factors are imposed on the HIV-1 proviruses, determining their transcriptional and latent fate. However, so far only limited host epigenetic regulators have been illustrated and studied in the context of HIV-1 latency. Identification of previously underappreciated LPGs contributing to epigenetic silencing of HIV-1 proviruses, and further investigation of their molecular mechanisms will not only improve our understanding of HIV-1 latent infection, but also facilitate the development of new strategies to tackle with latently infected HIV-1 proviruses by pharmacologically targeting the host epigenetic regulators. In this report, we identified the histone demethylase, MINA53 (MYC-induced nuclear antigen 53 kDa), as a potentially novel LPG from screening of the CRISPR/Cas9 sgRNA libraries particularly enriched with human nuclear proteins, and we further validated MINA53 using cell models of HIV-1 latency and investigated MINA53's underlying mechanisms involved in maintenance of HIV-1 latency.

MATERIALS AND METHODS

Antibodies, peptides and proteins

Antibodies against Histone H3 (39763), H3K36me3 (61021), H3K36me2 (61019), H3K27me3 (39155), H3K9me3 (61013), H3K4me3 (61379), MINA53 (61713) and KAT8 (61245) were from Active Motif. Antibody against H3K36me1 (ab9048) was from Abcam. Antibodies against KAT5 (sc-5725), GAPDH (sc-25778), as well as normal mouse IgG (sc-2025), normal rabbit IgG (sc-2027), goat anti-mouse IgG-HRP (sc-2005) and goat anti-rabbit IgG-HRP (sc-2004) antibodies were from Santa Cruz. Anti-acetyl-Histone H4 (Lys16) polyclonal antibody (07-329) was from Milipore. Recombinant histone peptides H3K36me3 (31580), H3K27me3 (31579), H3K9me3

(31279) and H3K4me3 (31278) were from Active Motif. MINA53 recombinant protein was from Novusbio (BP2-51814).

Cells

HIV-1 latency cell lines, J-LAT A2, L-LAT 10.6 and U1/HIV, were obtained from NIH AIDS reagent program, and cultured in RPMI-1640 medium with 10% FBS. Primary CD4 T cells were purchased from Lonza, and cultured in complete medium (RPMI-1640, 10% FBS, 1× glutamine, 1× MEM non-essential amino acid solution, 20 mM HEPES). HIV-1 reactivation in these cells was analyzed by flow cytometry (Accuri 6plus) for measuring GFP-positive cells or by qPCR for measuring Gag mRNA level.

CRISPR/Cas9 screen

Lentiviral sgRNA sub-library targeting nuclear proteins was acquired from Addgene (Cat. # 51047). The plasmid expressing Cas9 was a kind gift from Dr Joshua Munger (University of Rochester). For the CRISPR/Cas9 sgRNA screen, we followed the previously published protocol (15). Lentiviruses were packed in HEK293T cells using three-vector system including psPAX2, pMD2.G and lentiviral vectors expressing Cas9 or sgRNA sub-library. J-LAT A2 cells were transduced with lentiviruses expressing Cas9, followed by the puromycin selection for 4 days before its use for screen. Cas9 expression in J-LAT A2 cells was measured by qPCR (data not shown). J-LAT A2 cells stably expressing Cas9 were spin-inoculated with lentiviruses expressing sgRNA sub-library at the MOI of 0.3–0.5 in the presence of polybrene (8 µg/ml). At 7 days post transduction, GFP-positive cells were sorted. Both sorted and unsorted cells were harvested for extraction of genomic DNAs using the QIAmp® DNA Mini Kit (Qiagen). Nested PCRs were performed to amplify the sgRNA sequences, which was further processed for deep sequencing on HiSeq 2500 Sequencing System (Illumina) at University of Rochester Genomics Research Center. The sgRNA reads were further de-convoluted, and the abundance of each sgRNA (sorted/unsorted) was determined.

RNAi knockdown

siRNAs were used to transfect resting CD4 T cells. The control siRNA contains a pool of Silencer Negative siRNAs (Nos. 1–4, AM4611, AM4613, AM4615 and AM4641, Life Technologies). MINA53 siRNAs: siMINA53-1, 5'-GGG UCC CUG UUC AAG CUA A-3'; siMINA53-2, 5'-GAA CCA UUC AUC AAG CGG A-3' (Life Technologies). Gene-specific or non-targeting (NT) shRNAs were cloned into pAPM or pInducer10 lentiviral vector as previously described (16), using XhoI and EcoRI sites. These lentiviral vectors were packed into lentiviruses by cotransfection with psPAX2 and pMD2.G package vectors into HEK293T cells. pAPM lentiviruses were transduced into J-LAT A2, J-LAT 10.6 or U1/HIV cells, and pInducer10 lentiviruses into primary CD4 T cells, which were selected by puromycin. shRNA expression in pInducer10-transduced cells was induced by treating cells with doxycycline (0.1 µg/ml). Knockdown of shRNA-targeted genes

was measured by qPCR or immunoblotting. The gene-specific shRNAs are listed: Non-targeting (NT)-sh: 5'cacaacgctctcatcgacaag3'; KDM5A-sh: 5'cagcctctatttgcctgtga a3'; KDM1B-sh: 5'gcaagcaagattgcagtattt3'; MINA53-sh: 5'attggctcgaatgtgtacata3'; KDM4A-sh: 5'gccttgggtctttctgtg gat3'; UTY-sh: 5'gcgagcaaatagataattt3'; KAT8-sh: 5'aa agacagtgaaggatgctgta3'.

Quantitative PCR (qPCR)

To measure shRNA-mediated gene knockdown or HIV-1 proviral gene expression, total RNAs from the studied cells were isolated using Qiagen RNeasy Minikit (741014), and reverse-transcribed using iTaq™ Universal SYBR^R Green Supermix (Bio-Rad, 172-5121). The gene-specific primers were mixed with cDNA templates and iTaq™ Universal SYBR^R Green supermix (Bio-Rad). qPCR was carried out on the CFX Connect™ real-time PCR detection system (Bio-Rad) in a total volume of 20 µl. Relative fold change was determined by normalizing to GAPDH mRNA. For qPCR assays of ChIP samples, extracted DNA of each sample was mixed with HIV-1 LTR Nuc-1 primers. Relative fold enrichment was determined by normalizing to IgG control. The primers for qPCR are listed: KDM5A, F 5'caacgaaaggcactctctc3', R 5'caaagctctcgaggtttg3';

KDM1B, F 5'tacggcaacatgtctctgtgt3', R 5'aaccagtagggagt tgct3';

MINA53, F 5'gcaccaagaactgctttcc3', R 5'cggcagtactgtga ggaca3';

KDM4A, F 5'ttgcctggcacactgaagac3', R 5'tccagcctcttgagtc acct3';

UTY, F 5'cacctccaagaccaccaact3', R 5'ttttcatctgctggttgca g3';

KAT8, F 5'ggagaagccactgtctgacc3', R 5'gagggattgcaggga ctga3';

GAG, F 5'gacgctctcgaccatctc3', R 5'ctgaagcgcgcacggcaa 3';

Nuc-0, F 5'gaagggttaatttgggtccca3'; R 5' gatgcagctctcgggcca tg3';

Nuc-1, F 5'ctgggagctctctggctaacta3', R 5' ttaccagatcacaca acagacg3';

Nuc-2, F 5'atcttgactagcggaggcta-3'; R 5' acagcctctgatgtctc ta-3'.

Histone demethylation assay

Recombinant histone peptides were incubated with MINA53 recombinant protein in the demethylation buffer (50 mM Tris [pH 8.0], 50 mM KCl, 10 mM MgCl₂, 1 mM α-ketoglutarate, 40 µM FeSO₄, 2 mM ascorbic acid) at 37°C for 5 h (17). Reaction mixtures were mixed with 2× Laemmli Sample Buffer (Bio-Rad), and the aliquots were analyzed by SDS-PAGE and immunoblotting.

Chromatin immunoprecipitation (ChIP)

ChIP assays were performed as described previously (16). Cells were cross-linked by using 0.5% formaldehyde, followed by treating with 125 mM glycine to quench the reaction. After washing with cold 1× PBS, cells were lysed

for 10 min on ice in 1× CE buffer (10 mM HEPES-KOH [pH 7.9], 60 mM KCl, 1 mM EDTA, 0.5% Nonidet P-40, 1 mM DTT and protease inhibitor tablet). The nuclei were pelleted by centrifugation at 700 × g for 10 min at 4°C and re-suspended in 1× SDS lysis buffer (1% SDS, 10 mM EDTA, 50 mM Tris-HCl [pH 8.1] and protease inhibitor mixture). Nuclear lysates were sonicated for 2 min to fragment genomic DNAs, and subsequently diluted to 10-fold with 1× ChIP buffer (0.01% SDS, 1% Triton X-100, 1.2 mM EDTA, 16.7 mM Tris-HCl [pH 8.1], 150 mM NaCl and protease inhibitor mixture). The lysates were incubated for overnight at 4°C with specific antibodies or control mouse IgG or rabbit IgG. Protein A/G beads (Invitrogen) were pre-blocked with 0.5 mg/ml BSA and 0.125 mg/ml calf thymus DNA for 1 h at 4°C, and then added to the lysate-antibody mixture for another incubation at 4°C for 2 h. IPed samples were washed with the following buffers: low salt buffer (0.1% SDS, 1% Triton X-100, 2 mM EDTA, 20 mM Tris-HCl, pH 8.1, 150 mM NaCl); high-salt buffer (0.1% SDS, 1% Triton X-100, 2 mM EDTA, 20 mM Tris-HCl, pH 8.1, 500 mM NaCl); LiCl buffer (0.25 M LiCl, 1% NP-40, 1% Na-deoxycholate, 1 mM EDTA, 10 mM Tris-HCl [pH 8.1]); and 1× TE buffer (10 mM Tris-HCl [pH 8.1], 0.1 mM EDTA), and were eluted with 1× elution buffer (1% SDS, 0.1 M NaHCO₃) at room temperature. To reverse the cross-linking, the eluted samples were incubated at 65°C for overnight in the presence of 0.2 M NaCl. The eluted samples were then treated with proteinase K, and the DNA species were precipitated by using phenol-chloroform. The DNA pellets were re-suspended in water and quantified by qPCR. Input (1%) was used for qPCR analysis. The results were normalized to input values (percent input = $2^{[(C_{t, Input} - C_{t, IP}) \times 100]}$).

CD4 T-cell models of HIV-1 Latency

Two primary cell models of HIV-1 latency were used to determine MINA53's contribution to HIV-1 latency. One primary CD4 T cell model of HIV-1 latency was previously described by Vicente Planelles' group (16). dHIV-nef viral vector was a kind gift from Dr Vicente Planelles (University of Utah). Naïve CD4 T cells from healthy donors (Lonza) were stimulated with anti-human CD3 and CD28 antibodies (eBioscience) pre-coated on a Nunc-Immuno MaxiSorp plate (Thermo Scientific). Activated CD4 T cells were incubated with complete medium supplemented with 10 ng/ml of TGFβ, 2 µg/ml of anti-human IL-12 and 1 µg/ml of anti-human IL-4 (R&D Systems) for 3 days. These cells were spin-inoculated with pInducer10 lentiviruses at 1741 × g at 37°C for 2 h. Cells were re-suspended in complete medium supplemented with 100 IU/ml of rIL-2 and kept in culture for 4 days. On day 7, cells were infected with VSV-G pseudotyped dHIV-nef viruses and selected with puromycin (1 µg/ml). Cells were kept in culture for another 10 days and then treated with doxycycline (0.1 µg/ml) for 4 days to induce shRNA expression. On day 21, cells were collected and subjected to RNA extraction and RT-qPCR assays to quantify HIV-1 Gag RNAs. To determine the latency-reversing effect of JIB-04, the above CD4 T-cell model was used with slight modifications. Cells were infected with VSV-G pseudotyped dHIV-nef viruses and kept

in culture for 10 days, followed by the treatment with indicated compounds: JQ1 (1 μ M), JIB-04 (1 μ M), bryostatin-1 (10 nM), anti-CD3/CD28 antibodies (1:1) or DMSO. These compounds were used either alone or in combination. At 24-h post treatment, a portion of cells was aspirated for cell viability measurement while the compounds were removed from the remaining cells, which were re-suspended in the fresh complete RPMI media and kept in culture for another 3 days. These cells were subjected to the qPCR assay to quantify HIV-1 Gag mRNAs. We also employed another primary cell model established by Una O'Doherty's group with slight modification (18). Briefly, resting CD4 T cells were isolated from naïve primary CD4 T cells. Cells were cultured in the presence of IL-2 (30 U/ml) for 3 days, and then spinoculated with VSV-G pseudotyped dHIV-nef viruses at $1200 \times g$ for 2 h at 25°C. MINA53 siRNAs (siMINA53-1, siMINA53-2) or negative control siRNAs (siNT) were transfected into these cells via electroporation by using the recommended protocol (Neon Transfection System, Thermo Fisher). On day 3 post of transfection, cells were harvested and subjected to RNA extraction and RT-qPCR assays to quantify MINA53 or HIV-1 Gag RNAs. To evaluate the latency-reversing effect of JIB-04, the above resting CD4 T-cell model was also used. Cells were infected with VSV-G pseudotyped dHIV-nef viruses and kept in culture for 3 days. These HIV-infected cells will be treated with compounds and assayed similarly as in the Vicente Planelles model.

Ex vivo analysis using CD8-depleted PBMCs of aviremic patients

PBMCs were isolated from cART-treated, HIV-infected AIDS aviremic patients as previously described (16). Cells were cultured in the complete RPMI media with the presence of Nevirapine (600 nM) and IL-2 (30 IU/ml) for 3 days. CD8+ T cells were depleted by using the CD8 MicroBeads, human (Miltenyi Biotec). CD8-depleted PBMCs were treated with the indicated compounds: JQ1 (1 μ M), JIB-04 (1 μ M), bryostatin-1 (10 nM), anti-CD3/CD28 antibodies (1:1) or DMSO. These compounds were used either alone or in combination. At 24 h post treatment, a portion of cells was aspirated for cell viability measurement while the compounds were removed from the remaining cells, which were re-suspended in the fresh complete RPMI media and kept in culture for another 3 days. Supernatants were collected and subjected to the extraction of HIV viral RNAs by using the QIAmp[®] Viral RNA Kit (Qiagen). Nested qPCR assay was performed to quantify HIV viral RNAs as previously described (19). A serial dilution of HIV-1 IIIB viral RNAs with known concentration was used to establish standard curve for calculating the copy numbers of HIV viral RNAs in supernatant.

Cell viability assay

Cell viability was determined by measuring intracellular ATP level using Cell Titer Glo (Promega) or LIVE/DEAD[™] Fixable Far Red Dead Cell Stain Kit (for primary CD4 T cells or CD8-depleted PBMCs) as previously described (20).

RESULTS

CRISPR/Cas9 screen identifies novel nuclear proteins promoting HIV-1 latency

To further improve our understanding of host cellular machineries contributing to HIV-1 latency, we aimed to identify novel HIV-1 latency-promoting genes (LPGs) through the CRISPR/Cas9 functional genomic screens. We decided to initially focus on screening nuclear proteins since it is more likely that the host proteins residing in nucleus interfere with the transcriptional status of integrated HIV-1 proviruses. We utilized the sgRNA sub-pool library targeting nuclear proteins previously generated by Sabatini and Lander's groups (15). The screening strategy was illustrated (Figure 1A). The lentiviral pCW-Cas9 was transduced into J-LAT A2 cells harboring latently infected 'LTR-Tat-IRES-GFP' HIV-1 minigenome, and the stable cell line was selected by puromycin. Cells were further transduced with the lentiviral sub-pool libraries (10 sgRNAs per gene for 3733 nuclear proteins) for 7 days, followed by sorting GFP-positive cells indicating HIV-1 reactivation by flow cytometry. Un-sorted, GFP-negative cells were also harvested. Both GFP-positive and negative cell populations were subjected to genomic DNA extraction followed by PCR amplification of sgRNA barcodes. Barcode libraries were prepared for DNA deep sequencing. Abundance of each sgRNA in both GFP-positive and negative cell populations was deconvoluted, and its enrichment (GFP-positive versus negative) was determined. Presumably, sgRNA-mediated depletion of a LPG would result in the GFP expression so that the LPG's sgRNA shall be enriched in GFP-positive, i.e. HIV-reactivated cells.

The CRISPR/Cas9 screening results were processed using a comprehensive analysis pipeline, HiTSelect, which has demonstrated the superior performance on the data from both genome-wide RNAi and CRISPR/Cas9 screens (21). Genes were ranked according to their false-discovery rate (Fdr). In total, we identified 446 genes with $Fdr \leq 0.1$ (Figure 1B and Supplementary Table S1). Among them, most (394 out of 446) genes were scored with ≥ 2 active guide-RNAs. We next compared our screening results with previous datasets relevant to host-HIV interactions. A genome-wide shRNA screen of 19 056 genes was performed to identify host factors regulating HIV-1 latency and reactivation (22). From this screen, the total 2104 genes were claimed as the potential LPGs. About 51 genes were overlapped between our nuclear protein CRISPR screen (446 genes) and the above genome-wide shRNA screen (2104 genes), which is statically significant (P -value: 5.76×10^{-3}) from the hypergeometric simulation test (23) (Figure 1C and Supplementary Table S2). We also wondered whether our LPG candidates are involved in host-HIV protein-protein interactions (PPIs). From comparison of our nuclear protein CRISPR screen (446 genes) with 587 host-HIV literature-curated PPIs (VirusMint) as well as 522 host-HIV PPIs identified from a proteomic study (24), 21 LPG candidates involved in 23 known host-HIV PPIs were identified (Figure 1D and Supplementary Table S2). We further analyzed the pathway enrichment of our nuclear protein CRISPR screen (394 genes) using the Reactome database of bio-

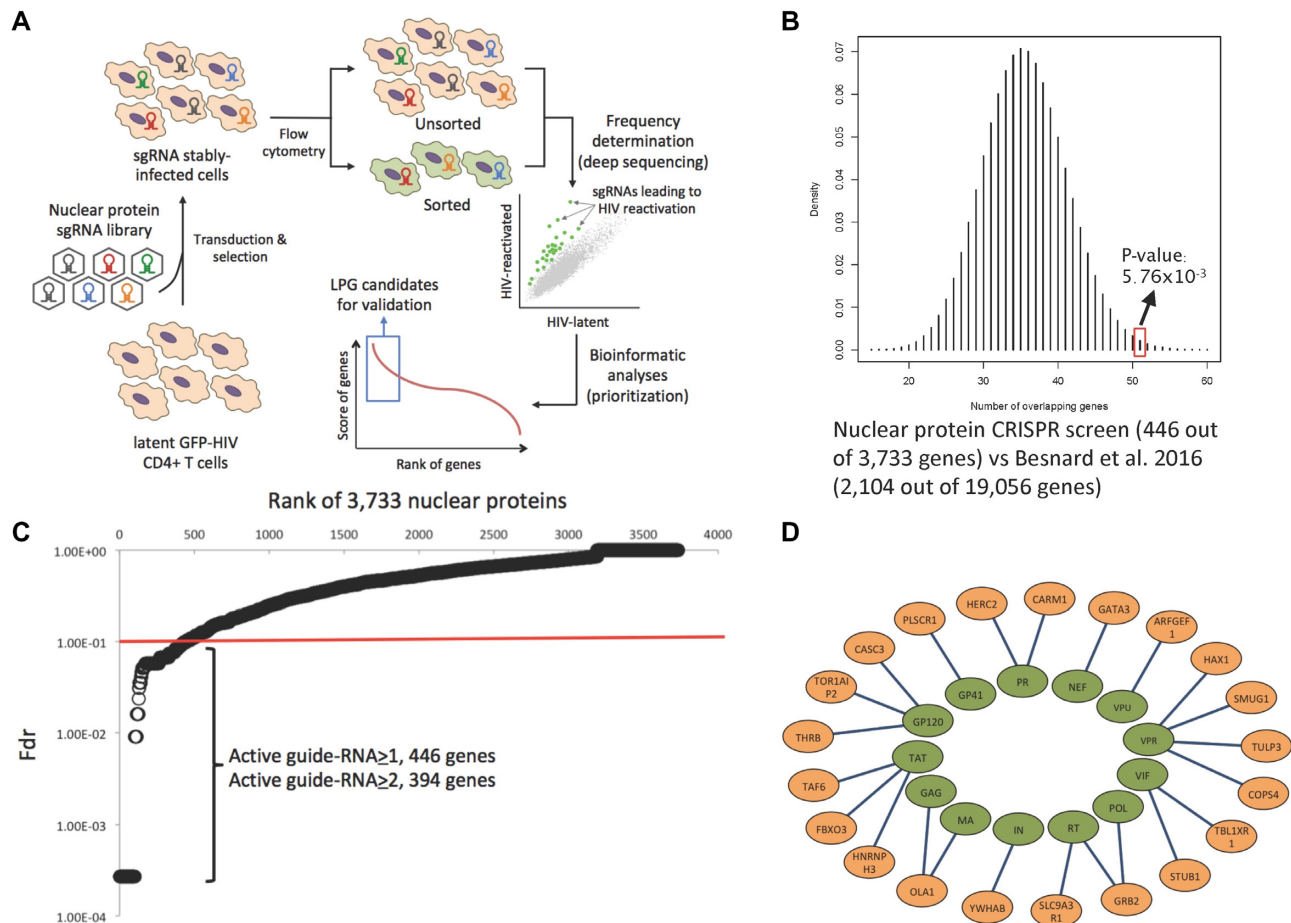


Figure 1. CRISPR/Cas9 screen identifies nuclear proteins promoting HIV-1 LPGs. (A) Scheme of CRISPR/Cas9 screen for identification of HIV-1 LPGs. Lentiviral sgRNA sub-library targeting nuclear proteins were transduced into J-LAT A2 cells stably expressing Cas9. At 7 days post transduction, GFP-positive cells were sorted. Both sorted and unsorted cells were harvested for extraction of genomic DNAs. sgRNA species were amplified and read through deep sequencing. The screen was independently repeated four times. The raw sgRNA reads were analyzed bioinformatically to identify LPG candidates for validation. (B) Rank of 3733 nuclear proteins from CRISPR/Cas9 screen was based on the value of false discovery rate (Fdr) calculated by HiTSelect for each gene according to its sgRNA reads. The Fdr of 446 genes were ≤ 0.1 , 394 genes of which were scored with ≥ 2 active guide-RNAs. (C) Hit comparison of our CRISPR/Cas9 nuclear protein screen with an earlier genome-wide shRNA screen yielded 51 overlapped LPGs with statistical significance from hypergeometric simulation test (P -value: 5.76×10^{-3}). (D) Hit comparison of our CRISPR/Cas9 nuclear protein screen with reported host-HIV protein-protein interaction (PPI) datasets yielded 21 overlapped host proteins that interact with at least one of HIV-1 viral proteins (total 23 PPIs).

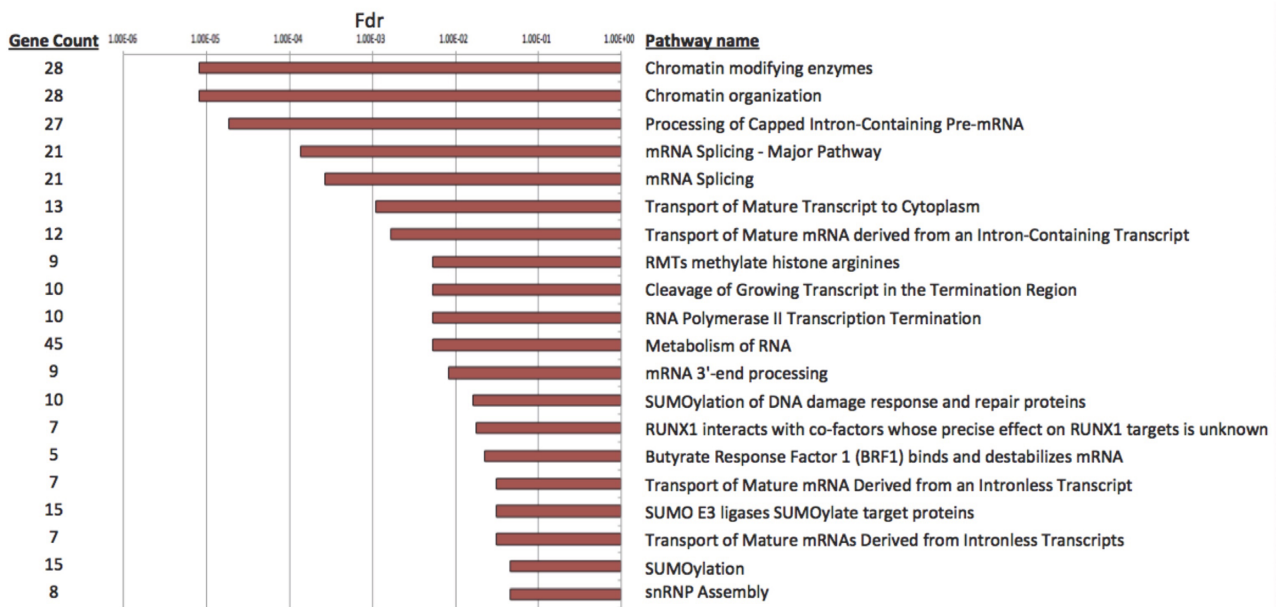
logical pathways. From the top 20 pathways (Figure 2A and Supplementary Table S3), the most significant two are 'chromatin modifying enzymes' and 'chromatin organization' (P -value: 1.69×10^{-8}). There were 28 nuclear proteins associated with these two pathways, which can be functionally cataloged in histone protein, acetylation/deacetylation, methylation/demethylation, and SWI/SNF complex (Figure 2B).

Verification of MINA53 as a potential LPG using multiple cell models

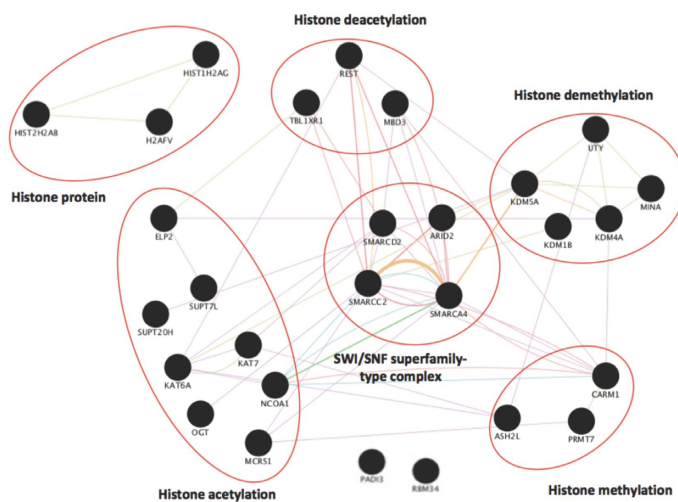
Our nuclear protein CRISPR screen suggests that a set of histone demethylases potentially promotes HIV-1 latency, which is surprising since the earlier studies showed that a set of counteracting enzymes, i.e. histone methyltransferases, also promotes HIV-1 latency (25–28). We further validated the significantly enriched histone demethylases (KDM1B, KDM4A, KDM5A, MINA53, UTY) by

alternative RNAi approach. Depletion of these histone demethylases by their shRNAs resulted in HIV-1 reactivation in J-LAT A2 cells comparing to the non-targeting (NT) shRNA (Figure 2C), while their expression was significantly reduced due to RNAi-mediated knockdown measured by qPCR (Figure 2D). KDM1B (LSD2) (29,30) and KDM5A (JARID5A) (31,32) are histone H3 lysine 4 (H3K4) demethylases catalyzing the active mark H3K4me3. KDM4A (JMJD2A) catalyzes H3K9me3 (inactive) and H3K36me3 (active) substrates (33,34). Similar as UTX (KDM6A), UTY (KDM6C) is male-specific lysyl demethylase catalyzing demethylation of H3K27me3 with reduced activity (35), but UTY was not well characterized as UTX that is required for Tat to remove the repressive mark H3K27me3 at LTR (36). MINA53 (MDIG, JMJD10) was suggested to demethylase H3K9me3 (37), but such activity was not observed in another earlier study (38). Given that MINA53 is a relatively less characterized histone

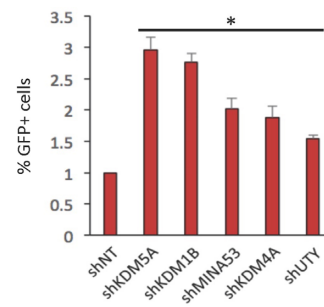
A



B



C



D

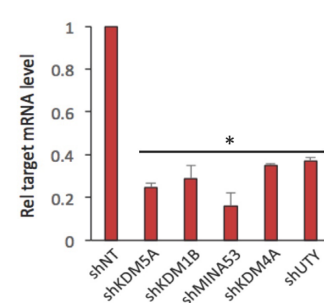


Figure 2. Histone demethylases are recognized as potential HIV-1 LPGs. (A) Top 20 pathways were significantly enriched for 394 LPG candidates with ≥ 2 active guide-RNAs, determined by Reactome pathway database. About 28 genes are involved in ‘chromatin modifying enzymes’ and ‘chromatin organization’ pathways. (B) Reactome analysis of 28 LPG candidates related to chromatin modification/organization further divided them into functional categories, including histone protein, histone acetylation/deacetylation, histone methylation/ demethylation, as well as SWI/SNF protein complex. (C and D) Validation of histone demethylases (HDMs) as HIV-1 LPGs by RNAi approach. J-LAT A2 cells stably expressing HDM-targeted shRNA (shKDM5A, shKDM1B, shKDM4A, shUTY, shMINA53) or non-targeting shRNA (shNT) were analyzed by flow cytometry to measure the percentage of GFP-positive cells (C) or by qPCR to measure the gene knockdown efficiency (D). All above results were normalized to shNT and presented as mean \pm SD from three independent experiments (* P -value < 0.05 , Student’s t -test).

demethylase and its function in HIV-1 replication was never reported, we focused on MINA53 for further investigation.

We first validated MINA53 in another two HIV-1 latency cell lines, J-LAT 10.6 and U1/HIV. Depletion of MINA53 by its shRNA significantly increases GFP-positive, i.e. HIV-activated, cell population in J-LAT 10.6 (Figure 3A) and HIV-1 Gag mRNA level in U1/HIV (Figure 3C) by 3–4 folds, while MINA53 shRNA significantly reduced MINA

expression in both cell lines through the measurement of its mRNA level by RT-qPCR (Figure 3B and D) or its protein level by immunoblotting (Supplementary Figure S2B). We also confirmed that MINA53 knockdown causes no obvious effect on cell viability in tested cells (Supplementary Figure S2D). Depletion of other histone demethylases (KDM1B, KDM5A) identified from the screen in J-LAT 10.6 and U1/HIV also caused HIV-1 reactivation (Supple-

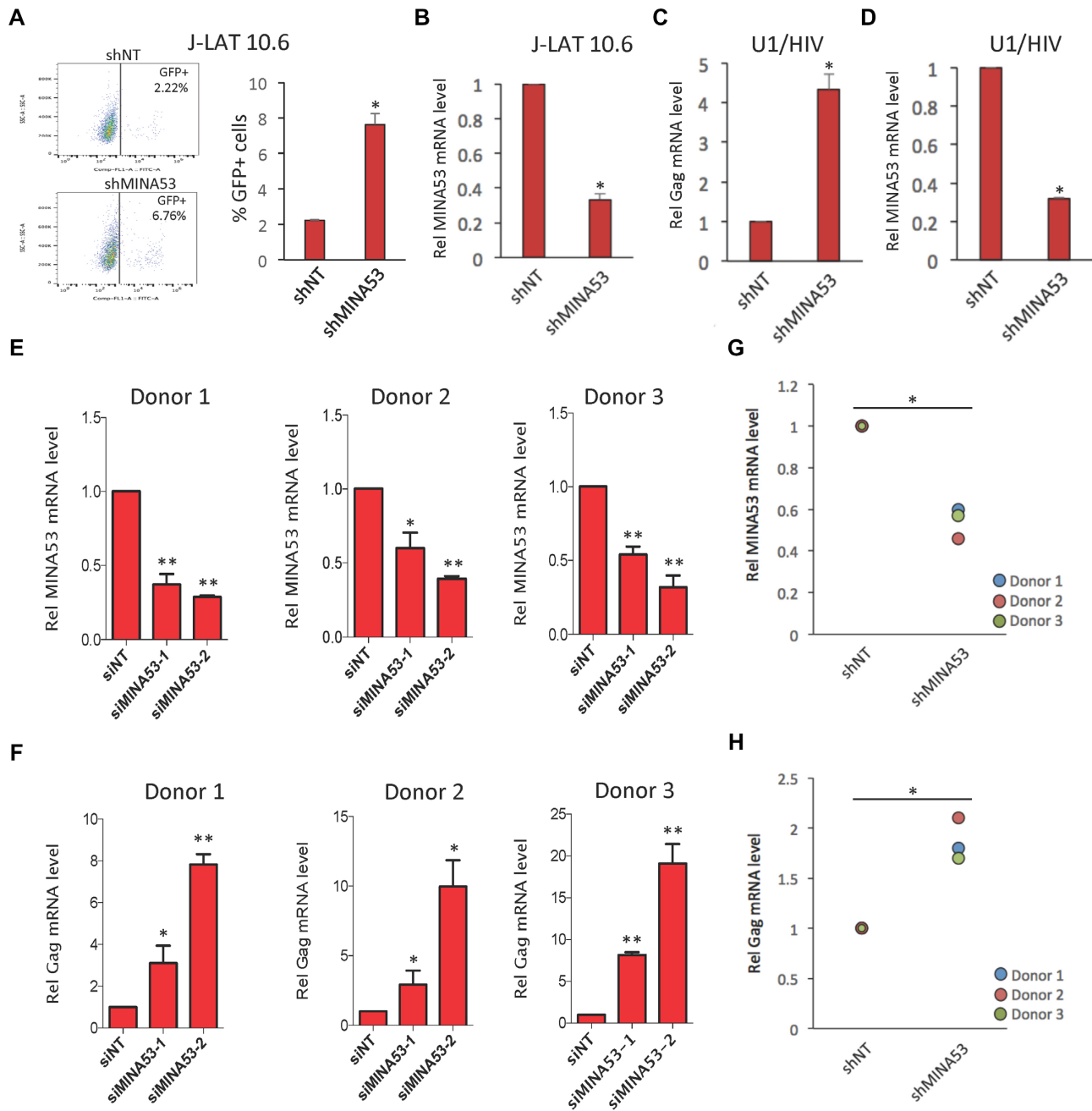


Figure 3. Loss of MINA53 reverses latent proviruses in cell models of HIV-1 latency. (A and B) J-LAT 10.6 cells stably expressing shMINA53 or shNT were analyzed by flow cytometry to measure the percentage of GFP-positive cells (A) or by qPCR to measure the MINA53 knockdown efficiency (B). Data were normalized to shNT samples. (C and D) U1/HIV cells stably expressing shMINA53 or shNT were analyzed by qPCR to measure HIV-1 Gag mRNA (C) or MINA53 knockdown efficiency (D). Data were normalized to shNT samples. All above results were presented as mean \pm SD from three independent experiments. (E and F) Resting CD4 T cells isolated from three donors (donors 1–3) were spinoculated with VSV-G pseudotyped dHIV-nef. Cells were transfected with siMINA53-1, siMINA53-2 or siNT. Total RNAs were extracted from these cells and analyzed by RT-qPCR to measure the mRNA level for MINA53 (E) or HIV-1 Gag (F). Data were normalized to siNT samples. All above results were presented as mean \pm SD from three independent experiments (* P -value < 0.05, ** P -value < 0.01, Student's t -test). (G and H) Primary CD4 T cells isolated from three donors (donors 1–3) were activated and transfected with doxycycline-inducible pInducer10 lentiviral vector expressing shMINA53 or shNT, followed by the infection of VSV-G pseudotyped dHIV-nef. Cells were kept in culture to allow HIV-1 proviruses enter latency. shRNA expression was induced by treating cells with doxycycline. Total RNAs were extracted and analyzed by qPCR to measure HIV-1 Gag mRNA (G) or MINA53 knockdown efficiency (H). Data were normalized to shNT samples and compared across three donors. (* P -value < 0.05, one-way ANOVA test).

mentary Figure S1). We second validated MINA53 in two primary CD4 T cell models of HIV-1 latency. We utilized the primary resting CD4 T-cell model of HIV-1 latency established by Una O'Doherty's group (18). Two MINA53 siRNAs (siMINA53-1 and siMINA53-2) or negative control siRNAs (siNT) were first verified in MAGI (HeLa-CD4-LTR- β -gal) cells in terms of their MINA53 knockdown efficiency (Supplementary Figure S2C), and then transfected into resting CD4 T cells harboring latent HIV-1 through electroporation. MINA53 or HIV-1 Gag mRNA level was measured by RT-qPCR. MINA53 knockdown by two siRNAs both moderately reduces MINA53 expression (Figure 3E) but dramatically increases HIV-1 gene expression (3–20 fold) across three donors as compared to siNT (Figure 3F). We also evaluated MINA53 using another primary CD4 T-cell model of HIV-1 latency previously described by Vicente Planelles' group (16). The pInducer10 lentiviral vector expressing MINA53 or NT shRNA was transduced to primary CD4 T cells isolated from three healthy donors and stably selected by puromycin. HIV-1 latency was established in the above shRNA-transduced CD4 T cells, followed by the induction of shRNA expression by treating cells with doxycycline. Both HIV-1 gene expression and MINA53 knockdown were measured by qPCR. Compared to NT shRNA, doxycycline-induced expression of MINA53 shRNA reduced ~50% of MINA53 expression in these cells (Figure 3G) but increased HIV-1 Gag mRNA level up to ~2-fold in all three donors (Figure 3H). In summary, our data showed that knockdown of MINA53 consistently reactivates latent HIV in multiple cell models of HIV latency.

MINA53 contributes to HIV-1 latency through demethylation of H3K36me3 at LTR

MINA53 is a known histone demethylase. Although it is not conclusive, MINA53 may target multiple methylated histone substrates. To sort out this issue, we performed the *in vitro* histone demethylation assays for MINA53, which would further improve our understanding of MINA53's role in HIV-1 latency. We found that recombinant MINA53 protein preferentially demethylates H3K36me3 even at the lower dose but a dose-dependent manner, while it marginally demethylated H3K9me3, a reported MINA53 histone substrate (39), at the higher dose (Figure 4A). These assays also showed that MINA53 failed to demethylate other tested histone substrates, H3K4me3 and H3K27me3 (Figure 4A).

We next determined whether depletion of MINA53 indeed increases the local H3K36me3 level at 5' LTR of integrated HIV-1 proviruses in J-LAT A2 cells by using CHIP-PCR assays. MINA53 protein level in J-LAT A2 cells stably expressing MINA53 or NT shRNA was determined by immunoblotting (Figure 4B), and these cells were lysed and subjected to crosslinking of protein–DNA complexes and immunoprecipitation of mono-, di- or tri-methylated H3K36 proteins (H3K36me1, me2 and me3) using their specific monoclonal antibodies. DNA species associated with methylated H3K36 immuno-complexes were extracted and analyzed by qPCR using the primers amplifying the

nuc-1 region of HIV-1 5' LTR. Depletion of MINA53 by RNAi significantly increased the level of H3K36me3 but reduced the level of H3K36me1 at nuc-1 (Figure 4C). We also determined whether depletion of MINA53 reduces the level of tri-methylated H3K4 and H3K9 (H3K4me3, H3K9me3) at 5' LTR nuc-1, but there was no obvious effect (Supplementary Figure S2). These results confirmed that MINA53 specifically regulates the methylation status of nucleosomal H3K36 at HIV-1 promoter.

We further determined whether the MINA53 association and the coordinated level of H3K36 methylation at LTR nuc-1 were dynamically regulated once HIV-1 was reactivated from latency. HIV-1 reactivation in J-LAT A2 cells was induced by TNF α or mock-treated, followed by the CHIP-PCR assays for MINA53 and methylated H3K36 proteins. The protein level of MINA53 is significantly reduced at 5' LTR nuc-1 in J-LAT A2 cells treated with TNF α to induce HIV-1 reactivation (Figure 4D), which also correlated with the significant increase of H3K36me3 but decrease of H3K36me1 at LTR nuc-1 (Figure 4E). MINA53 also associates with nuc-2 but not nuc-0, and similar to nuc-1 MINA53 dissociates from nuc-2 due to TNF α treatment (Figure 4D). These results suggest that the presence of MINA53 at HIV-1 promoter contributes to the H3K36 demethylation during latency but can be removed upon HIV-1 reactivation.

KAT8 recognizes H3K36me3 at 5' LTR and increases local level of H4K16ac

H3K36me3 is a histone marker associated with transcriptional activation, and one potential mechanism is that H3K36me3 has the cross-talk with another histone epigenetic mark H4K16ac in transcriptional regulation at HIV-1 promoter region, based on the earlier study of such cross-talk in the context of transcriptional elongation (40) and DNA damage repair (41). We determined whether such link also exists in the situation of HIV-1 reactivation. MINA53 depletion by RNAi led to the increased level of H4K16ac at 5' LTR nuc-1 (Figure 5A). TNF α treatment also caused the similar effect (Figure 5B). These results suggest that elevated H4K16ac at LTR nuc-1 correlates with the increase of H3K36 methylation due to MINA53 depletion or TNF α .

Certain histone acetyltransferases (HATs), such as KAT8 and KAT5, contain the chromodomains recognizing the methylated histones (42), and are known to mediate the acetylation of H4K16 (43,44). We then determined whether these chromodomain-containing HATs (KAT8, KAT5) are the epigenetic regulators that bridge the H3K36me3 and H4K16ac histone marks. The CHIP-PCR assay for KAT8 showed that the recruitment of KAT8 at LTR nuc-1 was strikingly increased due to MINA53 depletion in J-LAT A2 cells (Figure 5C), but there was no obvious increase of KAT5 (Supplementary Figure S3). TNF α treatment also led to a significant increase of KAT8 association at LTR nuc-1 (Figure 5D), suggesting that the higher level of H3K36 methylation due to the loss of MINA53 may facilitate the nucleosomal recruitment of KAT8 at HIV-1 promoter. Consistently, KAT8 shRNA reduced its expression (Figure 5E) and impaired the HIV-1 reactivation in J-

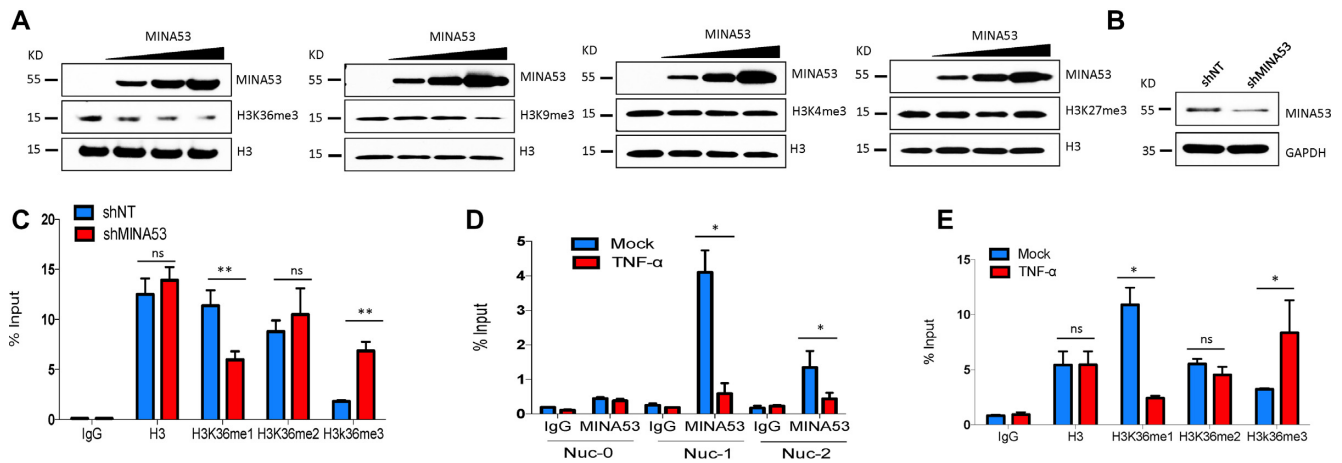


Figure 4. MINA53-mediated H3K36me3 demethylation correlates with HIV-1 reactivation. (A) *In vitro* histone demethylation assay of MINA53. Recombinant methylated histone H3 peptides (H3K36me3, H3K9me3, H3K4me3 or H3K27me3) were incubated with recombinant full-length MINA53 protein at increased doses. The reacted mixtures were separated on the SDS-PAGE gel, followed by the immunoblotting of MINA53, methylated and total H3 peptides, using their specific antibodies. (B and C) J-LAT A2 cells stably expressing shMINA53 or shNT were analyzed by protein immunoblotting to measure the MINA53 knockdown efficiency (B) or ChIP-PCR assay to measure the relative level of methylated (H3K36me1, H3K36me2 or H3K36me3) or total histone H3 peptides at HIV-1 5' LTR nucleosome nuc-1 (C), using their specific antibodies. (D and E) J-LAT A2 cells were treated with TNF α or mock treated, followed by the ChIP-PCR assay to measure the level of MINA53 at nucleosomes (nuc-0, nuc-1, nuc-2) around HIV-1 5' LTR (D) or methylated (H3K36me1, H3K36me2 or H3K36me3) or total histone H3 peptides at nuc-1 (E). All the ChIP-PCR results were normalized to the value from input (1%). All above results were presented as mean \pm SD from three independent experiments (* *P*-value < 0.05, ** *P*-value < 0.01, Student's *t*-test).

LATA2 cells induced by TNF α treatment (Figure 5F), indicating that KAT8 indeed has a supportive function in reversing HIV-1 from latency.

A pan jumonji histone demethylase inhibitor JIB-04 reverses HIV-1 latency

Since MINA53 belongs to the jumonji domain-containing histone demethylases, we then examined the pharmacological impact of a pan jumonji histone demethylase inhibitor, JIB-04, on HIV-1 latency. Using the ChIP-PCR assay, we confirmed that the level of H3K36me3 histone mark at 5' LTR nuc-1 was indeed increased due to JIB-04 treatment in J-LAT A2 cells (Figure 6A). Concurrently, treatment of JIB-04 enables the reversal of HIV-1 latency in multiple HIV-1 latency cell lines, including J-LAT A2, 10.6, J89GFP and U1/HIV (Figure 6B–E), in a dose-dependent manner, but shows mild cytotoxicity (Supplementary Figure S4). Furthermore, JIB-04 synergizes with other types of latency-reversing agents, Bryostatins-1 or JQ1, to reactivate latent HIV-1 in J-LAT 10.6 and J89GFP cells (Figure 6D and E), determined by using the Bliss independence model (45,46). If the synergy indicator (f_{xyO}/f_{xYP}) > 1, the LRA combination generates a synergetic effect. The synergy was also consistently observed when CD4 T cells harboring latent HIV-1 in two primary CD4 T-cell models, especially in the Una O'Doherty model, or CD8-depleted PBMCs from aviremic patients were treated with JIB-04 + JQ1 (Figure 6F and G; Supplementary Figure S5). All these data suggest that use of the pan jumonji histone demethylase inhibitor JIB-04 could potentially induce the hypermethylation of H3K36 and lead to the reversal of HIV-1 latency, which could involve the inhibition of MINA53.

DISCUSSION

Functional genomic screens are useful approaches to identify host factors playing a role in regulating viral replications, including RNAi and CRISPR/Cas9. Recently, shRNA screens have been accomplished to search for host factors regulating HIV-1 latency (22). From this study, the mTOR complex was identified as the facilitator of HIV-1 reactivation but no significant finding of latency-promoting genes (LPGs). By using the CRISPR/Cas9-based gene knockout strategy, we screened the sgRNA sub-libraries in J-LAT A2 cells, aiming to identify the previously unappreciated LPGs. We screened the sgRNAs targeting 3733 nuclear proteins, since this group of protein is likely enriched for epigenetic regulator of HIV-1 latency. From our nuclear protein CRISPR/Cas9 screen, we were able to identify a list of potential LPGs, which has the significant overlaps with the datasets from earlier studies of host factors that either regulate HIV-1 latency (Figure 1C) or associate with HIV-1 proteins (Figure 1D). Comparison of our LPG hit list with these reported datasets not only validates the success of our screen but also directs us to those overlapped hits for further investigation of their roles in HIV-1 latency. Multiple epigenetic players involved in the regulation of chromatin modification and organization, two of the top enriched pathways, have been identified from our screen as potential LPGs with statistical significance (Figure 2A and B). Some have been already implicated as facilitating HIV-1 latency. It has been reported that CARM1, a HMT, catalyzes the H3R26 arginine methylation and inactivates HIV-1 transcription (28). HDACs are known to silence HIV-1 proviruses (47,48), and the identified HDAC-associated proteins (REST, MBD3, TBL1XR1) could promote HIV-1 latency through the modulation of HDAC activities. Recently, it has been also reported that certain HATs also contributes to HIV-1 latency

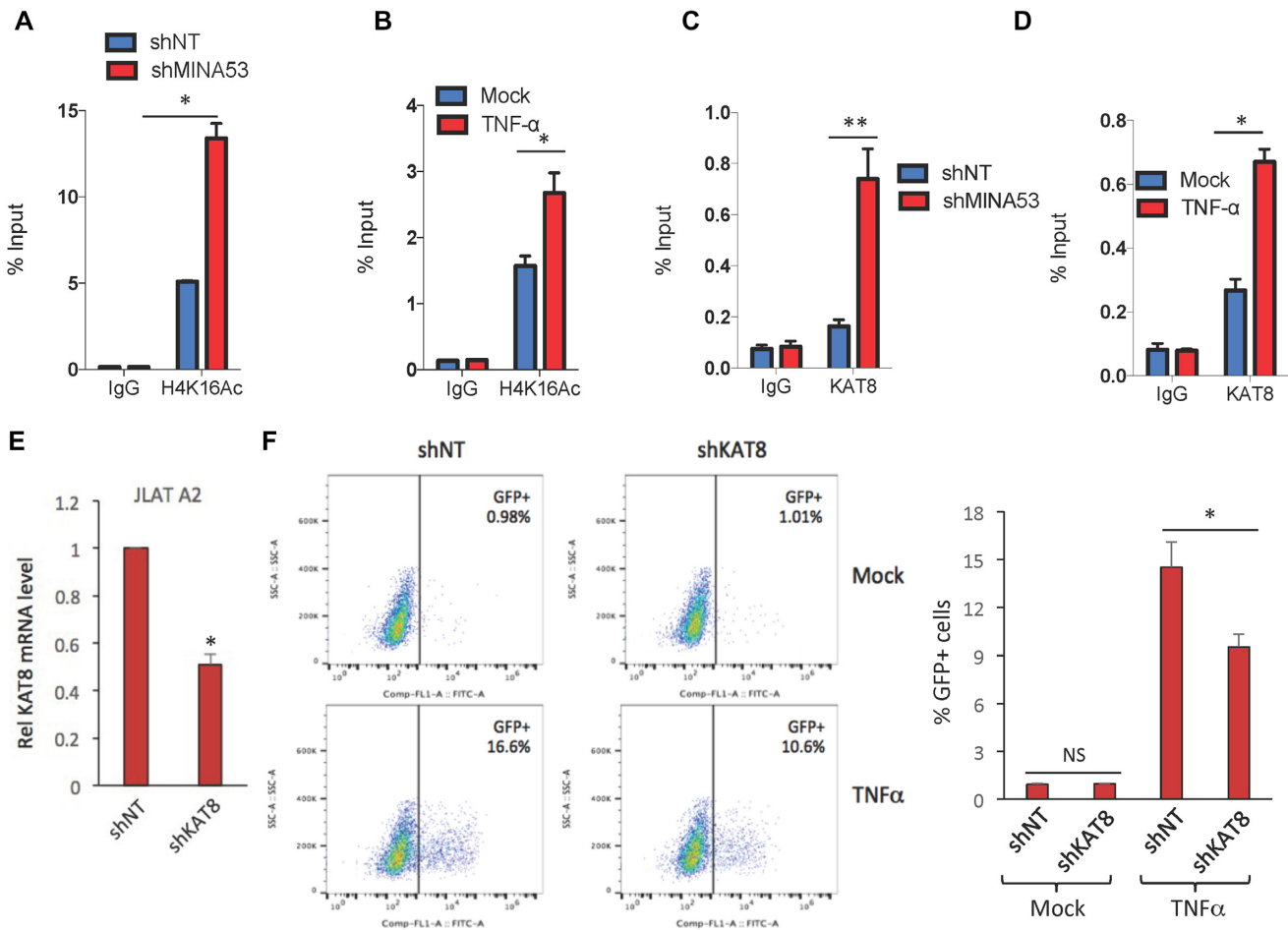


Figure 5. Loss of MINA53 enhances LTR association of KAT8 that mediates H4K16 acetylation. (A) J-LAT A2 cells stably expressing shMINA53 or shNT were analyzed by ChIP-PCR assay to measure the level of acetylated histone H4 peptide (H4K16ac) at HIV-1 5' LTR nucleosome nuc-1, using its specific antibody. (B) J-LAT A2 cells were treated with TNF α or mock treated, followed by the ChIP-PCR assay to measure the level of H4K16ac at HIV-1 5' LTR nucleosome nuc-1. (C and D) Similar as (A and B) but analyzed for the level of KAT8 at HIV-1 5' LTR nucleosome nuc-1. All the ChIP-PCR results were normalized to the value from input (1%). (E) J-LAT A2 cells stably expressing shKAT8 or shNT were analyzed by qPCR to measure the KAT8 knockdown efficiency. Data were normalized to shNT. (F) J-LAT A2 cells stably expressing shKAT8 or shNT were treated with TNF α (1 ng/ml) or mock treated, followed by the flow cytometry analysis to measure the percentage of GFP-positive cells. Data were normalized to mock-treated shNT samples. All above results were presented as mean \pm SD from three independent experiments (* P -value < 0.05, Student's t -test).

(49), explaining the legitimacy that we identified a set of HAT-related proteins from our screen.

However, it is quite surprising that a group of histone demethylases (KDM1B, KDM4A, KDM5A, MINA53, UTY) was enriched from our screens as LPGs (Figure 2B), since earlier studies showed that multiple histone methyltransferases, the counteracting enzymes of histone demethylases, facilitate HIV-1 latency. However, these results are not necessarily conflicting with each other but rather illustrate the complicated functions of histone methylation in the epigenetic regulation of HIV-1 latency. Methylations at different sites of histones at multiple degrees may correlate with either active or inactive status of HIV-1 proviral transcription. Various histone methyltransferases and demethylases can dynamically target these histone substrates and modulate their methylation levels, further complicating the impact of histone methylation on HIV-1 proviral transcription. Methylation can occur on multiple residues, including lysines, arginines and histidines, but

lysines (K) of histone tails H3 and H4 are the most common ones and well studied. In general, methylation of H3K27, H3K9 and H4K20 is associated with inactive gene expression, while methylation of H3K4, H3K36 and H3K79 is associated with active gene expression. In our case, we identified a set of histone demethylases that favor HIV-1 latency, likely due to that at least one of their substrates are active histone marks, which are either reported (H3K4me3: KDM1B, KDM5A; H3K36me3: KDM4A, MINA53) or remain to be identified in future (UTY).

The role of H3K36 methylation in HIV-1 latency is still not fully examined, and there were only limited results of this mark within the HIV-1 gene body (50). Dimethylated H3K36 (H3K36me2) on HIV-1 genes is induced upon TNF α activation in a P-TEFb-dependent manner (51). However, in a more recent study H3K36me2 seems not changed at the HIV-1 promoter upon TNF α activation (52). Trimethylated H3K36 (H3K36me3) was found across the transcribed region of HIV-1, mediated by Iws1, a protein

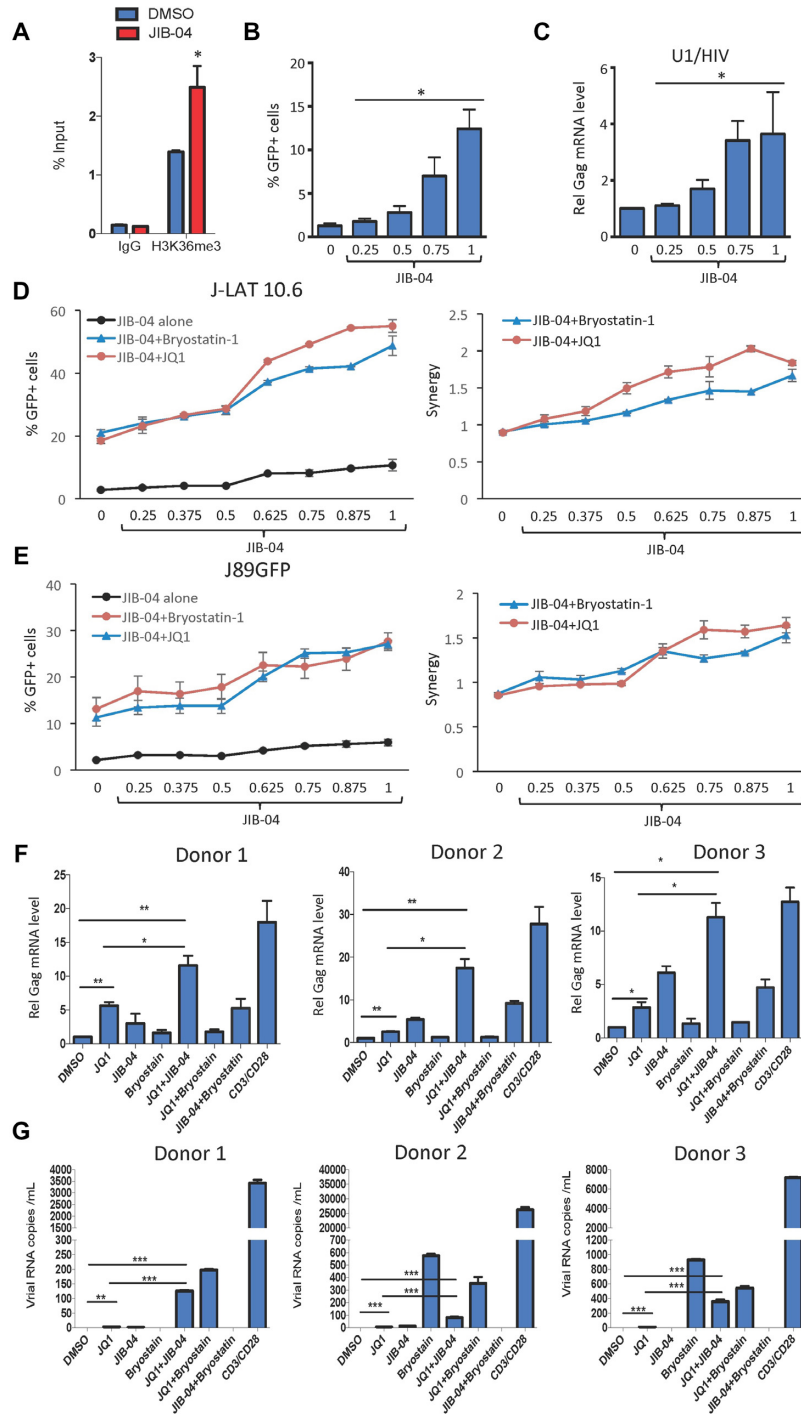


Figure 6. A pan jumonji histone demethylase inhibitor JIB-04 reverses HIV-1 latency. (A) J-LAT A2 cells were treated with JIB-04 (1 μM) or mock treated, followed by the ChIP-PCR assay to measure the relative level of H3K36me3 at HIV-1 5' LTR nucleosome nuc-1, using its specific antibody. All the ChIP-PCR results were normalized to the value from input (1%). (B and C) J-LAT A2 (B) or U1/HIV (C) cells were treated with JIB-04 (0.25-1 μM) or mock treated, followed by flow cytometry to measure the percentage of GFP-positive cells (J-LAT A2, B) or by qPCR to measure HIV-1 Gag mRNA (U1/HIV, C). Data were normalized to mock treatment. (D and E) J-LAT 10.6 (D) or J89GFP (E) cells were treated with JIB-04 (0.25-1 μM), alone or in combination with Bryostatatin-1(10 nM) or JQ1 (1 μM), or mock treated, followed by flow cytometry analysis to measure the percentage of GFP-positive cells (left panel). The synergy effect was calculated for combination of JIB-04 with Bryostatatin-1 or JQ1 by using the Bliss independence model (right panel). The LRA combination generates a synergistic effect if the synergy indicator $[f_{a_{xyO}}/f_{a_{xyP}}] > 1$. (F) Resting CD4 T cells isolated from three donors (donors 1-3) were spinoculated with VSV-G pseudotyped dHIV-nef. Cells were treated with the indicated compounds either alone or in combination: JQ1 (1 μM), JIB-04 (1 μM), Bryostatatin-1 (10 nM), anti-CD3/CD28 antibodies (1:1) or DMSO. Total RNAs were extracted and analyzed by RT-qPCR to measure HIV-1 Gag mRNA. Data were normalized to DMSO. (G) CD8-depleted PBMCs were isolated from three cART-treated, HIV-infected AIDS aviremic patients. Cells were treated with indicated compounds similar as (F). HIV-1 viral RNAs in the supernatants were extracted and quantified by the nested qPCR assay. Data were normalized to DMSO. All above results were presented as mean ± SD from three independent experiments (P -value: * < 0.05, ** < 0.05, *** < 0.001, Student's t -test).

binding to histone chaperone Spt6, which recruits the histone methyltransferase SETD2 to the RNAPII elongation complex (53). Interestingly, knockdown of Iws1 only decreases H3K36me3 across the transcribed region of HIV-1, but not the LTR promoter region, indicating that there is distinct regulation of this mark between HIV-1 gene body and promoter. Under this circumstance, our discovery of the histone demethylase MINA53 targeting H3K36me3 at HIV-1 promoter and contributing to HIV-1 latency is novel and the first report to link this epigenetic mark to HIV-1 latency. Our *in vitro* histone demethylation assay clearly confirmed that MINA53 preferentially demethylates the H3K36me3 substrate. The previous work illustrated that MINA53 weakly demethylates H3K9me3 as well (37), consistent with our assay showing that H3K9me3 was only demethylated when a high dose of recombinant MINA53 protein was used. Aligning with these results, we observed the dynamic change of methylation of H3K36 in HIV-1 latently infected cells due to MINA53 depletion or upon TNF α activation, reduction of H3K36me1 and increase of H3K36me3 at LTR nuc-1 (Figure 4C and E), but there is no change of H3K9me3 or H3K4me3 (Supplementary Figure S2). In addition, we observed that MINA53 knockdown yielded the better HIV-1 latency-reversing effect in primary cells using the Una O'Doherty model (Figure 3E and F), which could be explained by that HIV-1 latency established in resting CD4 T cells more physiologically mimics the natural HIV-1 reservoirs in cART-treated HIV patients.

Another significant finding is that MINA53-regulated H3K36me3 and KAT8-mediated H4K16Ac has a cross-talk at HIV-1 promoter to regulate HIV-1 latency (Figure 5). It was known that the cross-talk of H3K36me3 and H4K16ac play important roles in transcriptional regulation and DNA damage responses. For example, it was reported that H3K36me3 stimulates H4K16ac upon DNA double-strand break (DSB) induction in human cells, and DSB-induced H4K16ac was abolished upon depletion of STD2 (41). H4K16ac is generally considered as an active marker of transcription, and KAT8 and KAT5 are the two major histone acetyltransferases catalyzing the generation of H4K16ac (41,44,54,55). Both KAT8 and KAT5 contain the chromodomain that recognizes the methylated histones. However, the exact methylated histone marks that can be recognized by these HATs are not reported. Our results revealed that the increase of local H3K36me3 due to MINA53 depletion, leading to the significant increase of KAT8 occupancy (Figure 5C) but not KAT5 (Supplementary Figure S3) at LTR nuc-1, correlating with higher level of H4K16ac (Figure 5A). Our finding revealed a new epigenetic pathway at the promoter region that regulates HIV-1 latency. In our working model (Figure 7), we propose that the occupancy of MINA53 at the latent promoter is removed due to HIV-1 reactivation, leading to the increase of H3K36me3, which is subsequently recognized by KAT8 leading to the induction of H4K16ac, favoring HIV-1 transcription. These findings are important for understanding the epigenetic regulation of HIV-1 latency, and potentially the H3K36me3–H4K16ac axis can be targeted pharmacologically to eradicate latent HIV-1.

Thus, we tested the HIV-1 latency-reversing effect of a pan jumonji histone demethylase inhibitor JIB-04. Ear-

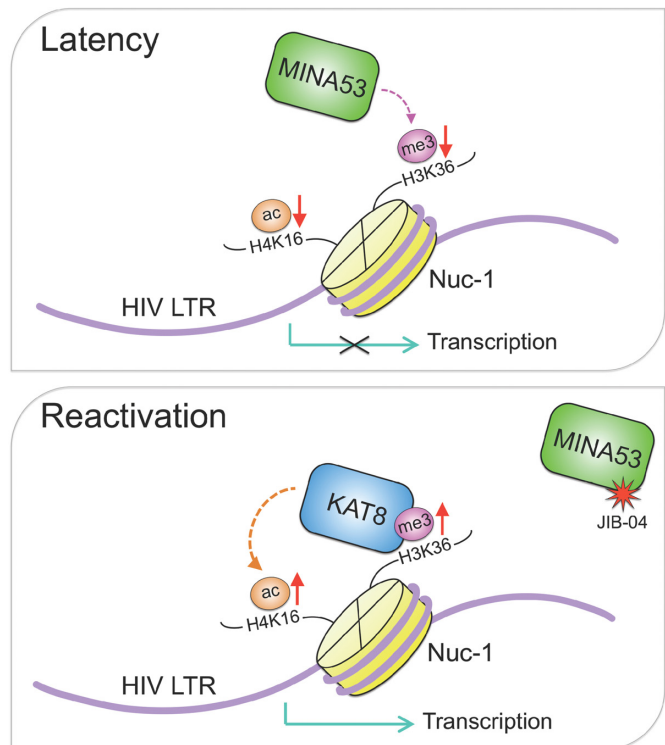


Figure 7. A proposed model describes MINA53's role in promoting HIV-1 latency. At the latent phase of HIV-1 infection, MINA53 occupies at the 5' LTR nucleosome nuc-1 of HIV-1 proviruses and constitutively demethylates the histone transcription-active marker, H3K36me3, which also correlates with the low level of another histone transcription-active marker, H4K16ac. Once latent HIV-1 proviruses are reversed due to TNF α treatment or use of the compound JIB-04, MINA53's histone demethylase activities are removed or inhibited, leading to the increase of H3K36me3 marker at 5' LTR nuc-1. One of the host HATs, KAT8, recognizes the elevated H3K36me3 at nuc-1 and catalyzes the acetylation of H4K16, which causes the increase of H4K16ac level at 5' LTR promoter and favors HIV-1 proviral transcription.

lier studies of JIB-04's anticancer activities demonstrated that JIB-04 selectively inhibits Jumonji demethylases over others *in vitro*, including DNA demethylase (TET1) and another type of histone demethylase (LSD1), and its inhibitory effect depends on the Jumonji levels in cells (15). Interestingly, JIB-04 was shown to inhibit enzymatic activities and cellular functions of KDM4A (56–59) and KDM5s (60,61), while both KDM4A and KDM5A were identified as potential LPGs from screens (Figure 2B). It is plausible since these jumonji histone demethylases, KDM4A and KDM5A, indeed catalyze the active marks H3K36me3 and H3K4me3 respectively, as one of their substrates (62).

Our results also showed that JIB-04 treatment increases the local H3K36me3 level at LTR nuc-1 (Figure 6A), further supporting the correlation of this mark with HIV-1 reactivation. The JIB-04 effect on the methylation of other histone sites at HIV-1 promoter and gene body needs further more profound analysis. Nevertheless, JIB-04 enables HIV-1 latency-reversal by itself (Figure 6B and C) or combined with other LRAs (Figure 6D–G). In particular, overall it is quite consistent that JIB-04 synergizes with JQ1 to reverse HIV-1 latency from latency T-cell lines (Figure

6D and E), primary cell models (Figure 6F, Supplementary Figure S5)—especially in the Una O’Doherty model, to reservoir cells from cART-treated HIV patients (Figure 6G). On the contrary, we observed that JIB-04 only synergizes with Bryostatins in latency T-cell lines (Figure 6D and E) but not in primary cells. This could be largely due to the difference between primary cells and immortalized T-cell lines in terms of many factors affecting HIV-1 proviral expression, such as transactivation signaling, chromatin status, cell proliferation and so on. An alternative explanation is that JIB-04+Bryostatins likely reactivates latent HIV-1 through certain common pathways while JIB-04+JQ1 through distinguished ones so that a synergy is generated in primary cells. This has been observed for other LRAs as well (46). Therefore, the synergy among LRAs really depends on cell types and varies across different cell systems of HIV-1 latency. Furthermore, a recent study suggested that JIB-04 (3 μ M) could inhibit Tat-mediated HIV-1 transcriptional elongation in 2D10 latency cell line, likely through increasing Tat K63-ubiquitylation and destruction via autophagy (63). It is curious that the authors found the effect of JIB-04 was not through putative histone demethylase targets. Such discrepancy indicates that JIB-04 may modulate HIV-1 proviral transcription more profoundly, depending on compound’s concentration, cellular heterogeneity or alternative targets. Above all, these results further illustrate the complicated role of histone methylation, involving multiple sites and degrees as well as many host methylation/demethylation enzymes, in regulating HIV-1 latency. In earlier studies, a set of inhibitors for histone methyltransferases was tested for their HIV-1 latency-reversing potency, including histone methyltransferase inhibitors (HMTis) for EZH2 (GSK-343, EPZ-6438) (25,26), G9a (UNC-0638, BIX01294) (25,64) and SUV39H1 (Chaetocin) (65)—all of these HMTs preferentially catalyze the suppressive marks (H3K27me3, H3K9me2-3). Given to the results of our studies, the compounds modulating histone methylation at HIV-1 latent promoters need to be carefully selected for the use of LRAs, ideally to only remove the inactive marks but reserve or boost the active marks at the same time.

SUPPLEMENTARY DATA

Supplementary Data are available at NAR Online.

ACKNOWLEDGEMENTS

We thank Dr. Una O’Doherty (University of Pennsylvania) for the invaluable guidance to employ the resting CD4 T-cell model of HIV-1 latency. We thank Dr. Vicente Planelles (University of Utah) for providing the dHIV-nef viral vector. We also thank the members of OSU Center for Retrovirus Research (Dr. Patrick Green, Dr. Shan-Lu Liu, Dr. Li Wu, Dr. Namal Liyanage and Dr. Amit Sharma) for helpful comments and feedback.

Author Contributions: J.Z. and N.S. conceived the study. H.H. and W.K. performed experiments. H.H., W.K., M.J., G.F., D.Z., T.H., J.Q., N.S. and J.Z. analyzed data and wrote the paper. J.Z. provided overall supervision of the study.

FUNDING

National Institutes of Health [R33AI116180, R01DE025447, R01GM117838 to J.Z.]. Funding for open access charge: National Institutes of Health [R33AI116180, R01DE025447 to J.Z.].

Conflict of interest statement. None declared.

REFERENCES

- Ruelas,D.S. and Greene,W.C. (2013) An integrated overview of HIV-1 latency. *Cell*, **155**, 519–529.
- Deeks,S.G. and Phillips,A.N. (2009) Clinical review: HIV infection, antiretroviral treatment, ageing, and non-AIDS related morbidity. *BMJ*, **338**, 288–292.
- Chomont,N., El-Far,M., Ancuta,P., Trautmann,L., Procopio,F.A., Yassine-Diab,B., Boucher,G., Boulassel,M.-R., Ghattas,G. and Brechley,J.M. (2009) HIV reservoir size and persistence are driven by T cell survival and homeostatic proliferation. *Nat. Med.*, **15**, 893–900.
- Darcis,G., Van Driessche,B. and Van Lint,C. (2017) HIV latency: Should we shock or lock? *Trends Immunol.*, **38**, 217–228.
- Yukl,S.A., Shergill,A., McQuaid,K., Gianella,S., Lampiris,H., Hare,C.B., Pandori,M., Sinclair,E., Günthard,H.F. and Fischer,M. (2010) Effect of raltegravir-containing intensification on HIV burden and T cell activation in multiple Gut sites of HIV+ adults on suppressive antiretroviral therapy. *AIDS*, **24**, 2451–2460.
- Wong,J.K., Hezareh,M., Günthard,H.F., Havlir,D.V., Ignacio,C.C., Spina,C.A. and Richman,D.D. (1997) Recovery of replication-competent HIV despite prolonged suppression of plasma viremia. *Science*, **278**, 1291–1295.
- Finzi,D., Hermankova,M., Pierson,T., Carruth,L.M., Buck,C., Chaisson,R.E., Quinn,T.C., Chadwick,K., Margolick,J. and Brookmeyer,R. (1997) Identification of a reservoir for HIV-1 in patients on highly active antiretroviral therapy. *Science*, **278**, 1295–1300.
- Chun,T.-W., Carruth,L., Finzi,D., Shen,X., DiGiuseppe,J.A., Taylor,H., Hermankova,M., Chadwick,K., Margolick,J. and Quinn,T.C. (1997) Quantification of latent tissue reservoirs and total body viral load in HIV-1 infection. *Nature*, **387**, 183–188.
- Archin,N.M., Sung,J.M., Garrido,C., Soriano-Sarabia,N. and Margolis,D.M. (2014) Eradicating HIV-1 infection: seeking to clear a persistent pathogen. *Nat. Rev. Microbiol.*, **12**, 750–764.
- Verdin,E., Paras,P. Jr and Van Lint,C. (1993) Chromatin disruption in the promoter of human immunodeficiency virus type 1 during transcriptional activation. *EMBO J.*, **12**, 3249–3259.
- Siliciano,R.F. and Greene,W.C. (2011) HIV latency. *Cold Spring Harb Perspect Med.*, **1**, a007096.
- Kumar,A., Darcis,G., Van Lint,C. and Herbein,G. (2015) Epigenetic control of HIV-1 post integration latency: implications for therapy. *Clin. Epigenetics*, **7**, 103.
- Van Lint,C., Emiliani,S., Ott,M. and Verdin,E. (1996) Transcriptional activation and chromatin remodeling of the HIV-1 promoter in response to histone acetylation. *EMBO J.*, **15**, 1112–1120.
- Margolis,D.M. (2011) Histone deacetylase inhibitors and HIV latency. *Curr. Opin. HIV AIDS*, **6**, 25–29.
- Wang,T., Wei,J.J., Sabatini,D.M. and Lander,E.S. (2014) Genetic screens in human cells using the CRISPR-Cas9 system. *Science*, **343**, 80–84.
- Huang,H., Santoso,N., Power,D., Simpson,S., Dieringer,M., Miao,H., Gurova,K., Giam,C.Z., Elledge,S.J. and Zhu,J. (2015) FACT proteins, SUPT16H and SSRP1, are transcriptional suppressors of HIV-1 and HTLV-1 that facilitate viral latency. *J. Biol. Chem.*, **290**, 27297–27310.
- Cloos,P.A., Christensen,J., Agger,K., Maiolica,A., Rappsilber,J., Antal,T., Hansen,K.H. and Helin,K. (2006) The putative oncogene GASC1 demethylates tri- and dimethylated lysine 9 on histone H3. *Nature*, **442**, 307–311.
- Pace,M.J., Graf,E.H., Agosto,L.M., Mexas,A.M., Male,F., Brady,T., Bushman,F.D. and O’Doherty,U. (2012) Directly infected resting CD4+T cells can produce HIV Gag without spreading infection in a model of HIV latency. *PLoS Pathog.*, **8**, e1002818.

19. Mousseau,G., Kessing,C.F., Fromentin,R., Trautmann,L., Chomont,N. and Valente,S.T. (2015) The tat inhibitor Didehydro-Cortistatin A prevents HIV-1 reactivation from latency. *mBio*, **6**, e00465.
20. Huang,H., Liu,S., Jean,M., Simpson,S., Huang,H., Merkley,M., Hayashi,T., Kong,W., Rodriguez-Sanchez,I., Zhang,X. *et al.* (2017) A novel bromodomain inhibitor reverses HIV-1 latency through specific binding with BRD4 to promote tat and P-TEFb association. *Front. Microbiol.*, **8**, 1035.
21. Diaz,A.A., Qin,H., Ramalho-Santos,M. and Song,J.S. (2015) HiTSelect: a comprehensive tool for high-complexity-pooled screen analysis. *Nucleic Acids Res.*, **43**, e16.
22. Besnard,E., Hakre,S., Kampmann,M., Lim,H.W., Hosmane,N.N., Martin,A., Bassik,M.C., Verschueren,E., Battivelli,E., Chan,J. *et al.* (2016) The mTOR complex controls HIV latency. *Cell Host Microbe*, **20**, 785–797.
23. Bushman,F.D., Malani,N., Fernandes,J., D’Orso,I., Cagney,G., Diamond,T.L., Zhou,H., Hazuda,D.J., Espeseth,A.S., Konig,R. *et al.* (2009) Host cell factors in HIV replication: meta-analysis of genome-wide studies. *PLoS Pathog.*, **5**, e1000437.
24. Jager,S., Cimermancic,P., Gulbahce,N., Johnson,J.R., McGovern,K.E., Clarke,S.C., Shales,M., Mercenne,G., Pache,L., Li,K. *et al.* (2012) Global landscape of HIV-human protein complexes. *Nature*, **481**, 365–370.
25. Nguyen,K., Das,B., Dobrowolski,C. and Karn,J. (2017) Multiple histone lysine methyltransferases are required for the establishment and maintenance of HIV-1 latency. *mBio*, **8**, e00133-17.
26. Tripathy,M.K., McManamy,M.E., Burch,B.D., Archin,N.M. and Margolis,D.M. (2015) H3K27 demethylation at the proviral promoter sensitizes latent HIV to the effects of vorinostat in *Ex vivo* cultures of resting CD4+ T cells. *J. Virol.*, **89**, 8392–8405.
27. Boehm,D., Jeng,M., Camus,G., Gramatica,A., Schwarzer,R., Johnson,J.R., Hull,P.A., Montano,M., Sakane,N., Pagans,S. *et al.* (2017) SMYD2-Mediated histone methylation contributes to HIV-1 latency. *Cell Host Microbe*, **21**, 569–579.
28. Zhang,Z., Nikolai,B.C., Gates,L.A., Jung,S.Y., Siwak,E.B., He,B., Rice,A.P., O’Malley,B.W. and Feng,Q. (2017) Crosstalk between histone modifications indicates that inhibition of arginine methyltransferase CARM1 activity reverses HIV latency. *Nucleic Acids Res.*, **45**, 9348–9360.
29. Ciccone,D.N., Su,H., Hevi,S., Gay,F., Lei,H., Bajko,J., Xu,G., Li,E. and Chen,T. (2009) KDM1B is a histone H3K4 demethylase required to establish maternal genomic imprints. *Nature*, **461**, 415–418.
30. Fang,R., Chen,F., Dong,Z., Hu,D., Barbera,A.J., Clark,E.A., Fang,J., Yang,Y., Mei,P., Rutenberg,M. *et al.* (2013) LSD2/KDM1B and its cofactor NPAC/GLYR1 endow a structural and molecular model for regulation of H3K4 demethylation. *Mol. Cell*, **49**, 558–570.
31. Zhou,X., Sun,H., Chen,H., Zavadil,J., Kluz,T., Arita,A. and Costa,M. (2010) Hypoxia induces trimethylated H3 lysine 4 by inhibition of JARID1A demethylase. *Cancer Res.*, **70**, 4214–4221.
32. Chaturvedi,C.P., Somasundaram,B., Singh,K., Carpenedo,R.L., Stanford,W.L., Dilworth,F.J. and Brand,M. (2012) Maintenance of gene silencing by the coordinate action of the H3K9 methyltransferase G9a/KMT1C and the H3K4 demethylase Jarid1a/KDM5A. *Proc. Natl. Acad. Sci. U.S.A.*, **109**, 18845–18850.
33. Whetstone,J.R., Nottke,A., Lan,F., Huarte,M., Smolnikov,S., Chen,Z., Spooner,E., Li,E., Zhang,G., Colaiacovo,M. *et al.* (2006) Reversal of histone lysine trimethylation by the JMJD2 family of histone demethylases. *Cell*, **125**, 467–481.
34. Black,J.C., Manning,A.L., Van Rechem,C., Kim,J., Ladd,B., Cho,J., Pineda,C.M., Murphy,N., Daniels,D.L., Montagna,C. *et al.* (2013) KDM4A lysine demethylase induces site-specific copy gain and rereplication of regions amplified in tumors. *Cell*, **154**, 541–555.
35. Walport,L.J., Hopkinson,R.J., Vollmar,M., Madden,S.K., Gileadi,C., Oppermann,U., Schofield,C.J. and Johansson,C. (2014) Human UTY(KDM6C) is a male-specific N-methyl lysyl demethylase. *J. Biol. Chem.*, **289**, 18302–18313.
36. Zhang,H.S., Du,G.Y., Liu,Y., Zhang,Z.G., Zhou,Z., Li,H., Dai,K.Q., Yu,X.Y. and Gou,X.M. (2016) UTX-1 regulates Tat-induced HIV-1 transactivation via changing the methylated status of histone H3. *Int. J. Biochem. Cell Biol.*, **80**, 51–56.
37. Huang,M.Y., Xuan,F., Liu,W. and Cui,H.J. (2017) MINA controls proliferation and tumorigenesis of glioblastoma by epigenetically regulating cyclins and CDKs via H3K9me3 demethylation. *Oncogene*, **36**, 387–396.
38. Williams,S.T., Walport,L.J., Hopkinson,R.J., Madden,S.K., Chowdhury,R., Schofield,C.J. and Kawamura,A. (2014) Studies on the catalytic domains of multiple JmjC oxygenases using peptide substrates. *Epigenetics*, **9**, 1596–1603.
39. Thakur,C. and Chen,F. (2015) Current understanding of mdig/MINA in human cancers. *Genes Cancer*, **6**, 288–302.
40. Bell,O., Wirbelauer,C., Hild,M., Scharf,A.N., Schwaiger,M., MacAlpine,D.M., Zilbermann,F., van Leeuwen,F., Bell,S.P., Imhof,A. *et al.* (2007) Localized H3K36 methylation states define histone H4K16 acetylation during transcriptional elongation in *Drosophila*. *EMBO J.*, **26**, 4974–4984.
41. Li,L. and Wang,Y. (2017) Cross-talk between the H3K36me3 and H4K16ac histone epigenetic marks in DNA double-strand break repair. *J. Biol. Chem.*, **292**, 11951–11959.
42. Yap,K.L. and Zhou,M.M. (2011) Structure and mechanisms of lysine methylation recognition by the chromodomain in gene transcription. *Biochemistry*, **50**, 1966–1980.
43. Thomas,T., Dixon,M.P., Kueh,A.J. and Voss,A.K. (2008) Mof (MYST1 or KAT8) is essential for progression of embryonic development past the blastocyst stage and required for normal chromatin architecture. *Mol. Cell Biol.*, **28**, 5093–5105.
44. Renaud,E., Barascu,A. and Rosselli,F. (2016) Impaired TIP60-mediated H4K16 acetylation accounts for the aberrant chromatin accumulation of 53BP1 and RAP80 in Fanconi anemia pathway-deficient cells. *Nucleic Acids Res.*, **44**, 648–656.
45. Hashemi,P., Barreto,K., Bernhard,W., Lomness,A., Honson,N., Pfeifer,T.A., Harrigan,P.R. and Sadowski,I. (2018) Compounds producing an effective combinatorial regimen for disruption of HIV-1 latency. *EMBO Mol. Med.*, **10**, 160–174.
46. Jiang,G., Mendes,E.A., Kaiser,P., Wong,D.P., Tang,Y., Cai,I., Fenton,A., Melcher,G.P., Hildreth,J.E., Thompson,G.R. *et al.* (2015) Synergistic reactivation of latent HIV expression by Ingenol-3-Angelate, PEP005, Targeted NF- κ B signaling in combination with JQ1 induced p-TEFb activation. *PLoS Pathog.*, **11**, e1005066.
47. Keedy,K.S., Archin,N.M., Gates,A.T., Espeseth,A., Hazuda,D.J. and Margolis,D.M. (2009) A limited group of class I histone deacetylases acts to repress human immunodeficiency virus type 1 expression. *J. Virol.*, **83**, 4749–4756.
48. Archin,N.M., Kirchherr,J.L., Sung,J.A., Clutton,G., Sholtis,K., Xu,Y., Allard,B., Stuelke,E., Kashuba,A.D., Kuruc,J.D. *et al.* (2017) Interval dosing with the HDAC inhibitor vorinostat effectively reverses HIV latency. *J. Clin. Invest.*, **127**, 3126–3135.
49. Li,Z., Mbonye,U., Feng,Z., Wang,X., Gao,X., Karn,J. and Zhou,Q. (2018) The KAT5-Acetyl-Histone4-Brd4 axis silences HIV-1 transcription and promotes viral latency. *PLoS Pathog.*, **14**, e1007012.
50. Turner,A.W. and Margolis,D.M. (2017) Chromatin regulation and the histone code in HIV latency. *Yale J. Biol. Med.*, **90**, 229–243.
51. Zhou,M., Deng,L., Lacoste,V., Park,H.U., Pumfery,A., Kashanchi,F., Brady,J.N. and Kumar,A. (2004) Coordination of transcription factor phosphorylation and histone methylation by the P-TEFb kinase during human immunodeficiency virus type 1 transcription. *J. Virol.*, **78**, 13522–13533.
52. Boehm,D. and Ott,M. (2017) Host methyltransferases and Demethylases: Potential new epigenetic targets for HIV cure strategies and beyond. *AIDS Res. Hum. Retroviruses*, **33**, S8–S22.
53. Yoh,S.M., Lucas,J.S. and Jones,K.A. (2008) The Iws1:Spt6:CTD complex controls cotranscriptional mRNA biosynthesis and HYPB/Setd2-mediated histone H3K36 methylation. *Genes Dev.*, **22**, 3422–3434.
54. Wu,J., Chen,Y., Lu,L.Y., Wu,Y., Paulsen,M.T., Ljungman,M., Ferguson,D.O. and Yu,X. (2011) Chfr and RNF8 synergistically regulate ATM activation. *Nat. Struct. Mol. Biol.*, **18**, 761–768.
55. Sun,Y., Jiang,X., Xu,Y., Ayrapetov,M.K., Moreau,L.A., Whetstone,J.R. and Price,B.D. (2009) Histone H3 methylation links DNA damage detection to activation of the tumour suppressor Tip60. *Nat. Cell Biol.*, **11**, 1376–1382.
56. Van Rechem,C., Black,J.C., Boukhali,M., Aryee,M.J., Graslund,S., Haas,W., Benes,C.H. and Whetstone,J.R. (2015) Lysine demethylase KDM4A associates with translation machinery and regulates protein synthesis. *Cancer Discover.*, **5**, 255–263.

57. Cascella,B., Lee,S.G., Singh,S., Jez,J.M. and Mirica,L.M. (2017) The small molecule JIB-04 disrupts O₂ binding in the Fe-dependent histone demethylase KDM4A/JMJD2A. *Chem. Commun.*, **53**, 2174–2177.
58. Mar,B.G., Chu,S.H., Kahn,J.D., Krivtsov,A.V., Koche,R., Castellano,C.A., Kotlier,J.L., Zon,R.L., McConkey,M.E., Chabon,J. *et al.* (2017) SETD2 alterations impair DNA damage recognition and lead to resistance to chemotherapy in leukemia. *Blood*, **130**, 2631–2641.
59. Wang,X., Wang,S., Yao,G., Yu,D., Chen,K., Tong,Q., Ye,L., Wu,C., Sun,Y., Li,H. *et al.* (2017) Identification of the histone lysine demethylase KDM4A/JMJD2A as a novel epigenetic target in M1 macrophage polarization induced by oxidized LDL. *Oncotarget*, **8**, 114442–114456.
60. Horton,J.R., Engstrom,A., Zoeller,E.L., Liu,X., Shanks,J.R., Zhang,X., Johns,M.A., Vertino,P.M., Fu,H. and Cheng,X. (2016) Characterization of a linked jumonji domain of the KDM5/JARID1 family of histone H3 lysine 4 demethylases. *J. Biol. Chem.*, **291**, 2631–2646.
61. Xu,W., Zhou,B., Zhao,X., Zhu,L., Xu,J., Jiang,Z., Chen,D., Wei,Q., Han,M., Feng,L. *et al.* (2018) KDM5B demethylates H3K4 to recruit XRCC1 and promote chemoresistance. *Int. J. Biol. Sci.*, **14**, 1122–1132.
62. Black,J.C., Van Rechem,C. and Whetstine,J.R. (2012) Histone lysine methylation dynamics: establishment, regulation, and biological impact. *Mol. Cell*, **48**, 491–507.
63. Xu,M., Moresco,J.J., Chang,M., Mukim,A., Smith,D., Diedrich,J.K., Yates,J.R. 3rd and Jones,K.A. (2018) SHMT2 and the BRCC36/BRISC deubiquitinase regulate HIV-1 Tat K63-ubiquitylation and destruction by autophagy. *PLoS Pathog.*, **14**, e1007071.
64. Imai,K., Togami,H. and Okamoto,T. (2010) Involvement of histone H3 lysine 9 (H3K9) methyltransferase G9a in the maintenance of HIV-1 latency and its reactivation by BIX01294. *J. Biol. Chem.*, **285**, 16538–16545.
65. Bernhard,W., Barreto,K., Saunders,A., Dahabieh,M.S., Johnson,P. and Sadowski,I. (2011) The Suv39H1 methyltransferase inhibitor chaetocin causes induction of integrated HIV-1 without producing a T cell response. *FEBS Lett.*, **585**, 3549–3554.